TURBULENT FLOW AND HEAT TRANSFER CHARACTERISTICS IN U-TUBES: A NUMERICAL STUDY

by

Khalid N. ALAMMAR

Original scientific paper
UDC: 536.24:532.517.4:519.61
DOI: 10.2298TSCI0904175A

Using the standard k-ε model, 3-dimensional turbulent flow and heat transfer characteristics in U-tubes are investigated. Uncertainty is approximated using experimental correlations and grid independence study. Increasing the Dean number is shown to intensify a secondary flow within the curved section. The overall Nusselt number for the tube is found to decrease substantially relative to straight tubes, while the overall skin friction coefficient remains practically unaffected. Local skin friction coefficient, Nusselt number, and wall temperature along the tube wall are presented.

Key words: *Dean number, friction, heat, numerical, U-tubes, turbulence*

Introduction

Due to secondary motion caused by the centrifugal force, curved tubes have been known to enhance heat and mass transfer. As such, they are being used extensively in heat exchangers and process industry. Examples of curved tubes include the helically coiled, spirally coiled, S-tubes, U-tubes, and others. Coiled tubes have received much attention as revealed in the review study by Naphon *et al*. [1]. However, and due to turbulence complexities, mainly laminar flows have been investigated, albeit in detail, *e. g.* [2, 3]

In addition to the secondary flow present in curved tubes, turbulence poses another challenge to the analysts and experimentalists alike. Hence, few attempts have been made in the past to investigate turbulent flows in curved tubes, and mainly at low Reynolds numbers. For example, Huttl *et al*. [4] investigated turbulent flow characteristics in curved and coiled tubes using direct numerical solution. They reported that torsional effects are much smaller than the curvature effects on the mean axial velocity. Nonetheless, they cannot be neglected because they have stronger influence on the secondary flow. Li *et al*. [5] used the renormalization group (RNG) k-ε model to investigate the mixed convective heat transfer in the entrance region of a curved pipe. They reported that the peripherally averaged Nusselt number and friction factor exhibit oscillatory behavior along the streamwise direction, and that the average Nusselt number and friction factor resulting from buoyancy was prominent at the entrance region of the pipe. In another study, Yang *et al*. [6] experimentally investigated effects of the Dean, Prandtl, and Reynolds numbers on flow and heat transfer characteristics in wavy tubes. They reported that higher Dean numbers result in higher heat transfer rate and friction.

Despite their practical importance in high performance heat exchangers, U-tubes have received relatively less attention. Unlike curved tubes, U-tubes are predominantly straight. Nevertheless, the curvature is expected to influence flow and heat transfer characteristics downstream of

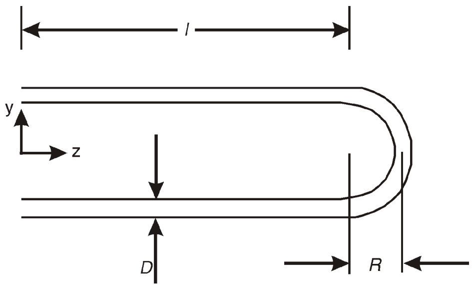

Figure 1. Schematic of the U-tube (y-z plane)

the curvature. In this work, a developing, 3-D, steady turbulent flow in a U-tube is simulated. The study is conducted for three Dean numbers, namely 2.0, 3.0, and $4.0 \cdot 10^4$. Schematic of the U-tube is shown in fig. 1. Here, l is length of the straight section (= 1.0 m), R – the radius of curvature (= 25 mm), and D – the tube diameter (= 20 mm).

The mathematical model

The mathematical model consisted of the following steady Reynolds-averaged conservation equations in Cartesian index form.

Continuity equation

$$\frac{\partial (\rho U_i)}{\partial x_i} \quad 0 \tag{1}$$

Momentum equations

$$\frac{\partial (\rho U_i U_j)}{\partial x_j} \qquad \frac{\partial p}{\partial x_i} \quad \frac{\partial}{\partial x_j} \ \mu \ \frac{\partial U_i}{\partial x_j} \quad \frac{\partial U_j}{\partial x_i} \quad \frac{2}{3}\delta_{ij} \frac{\partial U_i}{\partial x_i} \qquad \frac{\partial}{\partial x_j}(\quad \rho \overline{u_i u_j}) \tag{2}$$

For the Reynolds stresses, the Boussinesq hypothesis [7] was invoked:

$$\rho \overline{u_i u_j} \quad \mu_{\mathrm{t}} \quad \frac{\partial U_i}{\partial x_j} \quad \frac{\partial U_j}{\partial x_i} \qquad \frac{2}{3} \quad \rho k \quad \mu_{\mathrm{t}} \frac{\partial U_i}{\partial x_i} \ \delta_{ij} \tag{3}$$

Energy equation

$$\frac{\partial [U_i (\rho E \quad p)]}{\partial x_i} \qquad \frac{\partial}{\partial x_j} \quad K \quad \frac{c_{\mathrm{p}} \mu_{\mathrm{t}}}{\mathrm{Pr}_{\mathrm{t}}} \quad \frac{\partial T}{\partial x_j} \tag{4}$$

Turbulence model

The standard k-ε turbulence model [8] was used. The model is well suited for high Reynolds number internal flows and has been validated for many industrial flows.

$$\frac{\partial (\rho k U_i)}{\partial x_i} \quad \frac{\partial}{\partial x_j} \quad \mu \quad \frac{\mu_{\mathrm{t}}}{\sigma_{\mathrm{k}}} \quad \frac{\partial k}{\partial x_j} \qquad G_{\mathrm{k}} \quad \rho \varepsilon \tag{5}$$

$$\frac{\partial (\rho \varepsilon U_i)}{\partial x_i} \quad \frac{\partial}{\partial x_j} \quad \mu \quad \frac{\mu_t}{\sigma_\varepsilon} \quad \frac{\partial \varepsilon}{\partial x_j} \qquad C_{1\varepsilon} \frac{\varepsilon}{k} G_k \quad C_{2\varepsilon} \rho \frac{\varepsilon^2}{k} \tag{6}$$

Here, $C_{1\varepsilon}$ = 1.44 and $C_{2\varepsilon}$ = 1.92. Production of turbulence kinetic energy is given by:

$$G_{\mathrm{k}} \quad \rho \overline{u_i u_j} \frac{\partial U_j}{\partial x_i} \tag{7}$$

and the eddy viscosity is:

$$\mu_{\mathrm{t}} \quad \rho C_\mu \frac{k^2}{\varepsilon} \tag{8}$$

where $C_\mu = 0.09$.

Wall treatment

The standard wall function was implemented. For more details, the reader is referred to Fluent 6.3 user guide.

The numerical procedure

Fluent 6.3 was used as the solver. The grid was built using Gambit 2.0. The mesh consisted of approximately 300,000 cells, the radial distribution of which is shown in fig. 2. The simulation was carried out using SIMPLE calculation algorithm [9] and second-order differencing schemes. The linearized equations were solved using Gauss-Seidel method, in conjunction with an algebraic Multigrid scheme [10]. Turbulence intensity of 5%, hydraulic diameter of 0.02 m, and uniform temperature of 300 K were applied at the inlet. A uniform heat flux of 1000 W/m^2 was applied at the wall. Due to small overall temperature changes, fluid properties were assumed constant.

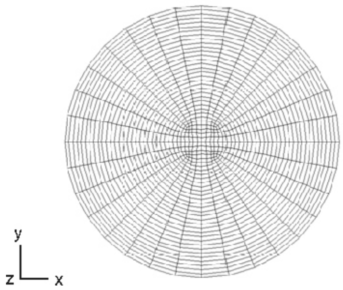

Figure 2. Mesh at a cross-section of the U-tube (x-y plane)

Uncertainty analysis

There are mainly two sources of uncertainty in CFD, namely modeling and numerical [11]. Modeling uncertainty can be approximated through experimental validation while numerical uncertainty can be approximated through grid independence. Numerical uncertainty has two main sources, namely truncation and round-off errors. Higher order schemes have less truncation error, and as was outlined earlier, the discretization schemes invoked were second-order. In explicit schemes, round-off error increases with increasing iterations, and is reduced by increasing significant digits (machine precision). However, having used Gauss-Seidel iterative procedure in a steady-state simulation renders the calculation insensitive to round-off error.

A comparison between the current simulation and Blasius correlation is depicted in fig. 3. The numerical prediction with 300.000 cells is in good agreement with the correlation except in the entrance region. Therefore, we assume that the modeling uncertainty is determined by the correlation uncertainty, which is assumed to be 5%. The numerical error is approximated by the difference between 20.000 and 30.000 cells, which is about 2% in the entrance region. Hence, we conclude that the overall friction uncertainty is determined by the modeling uncertainty, *i. e.* 5%. Similarly, it is shown in fig. 4 that uncertainty in the heat transfer is within un-

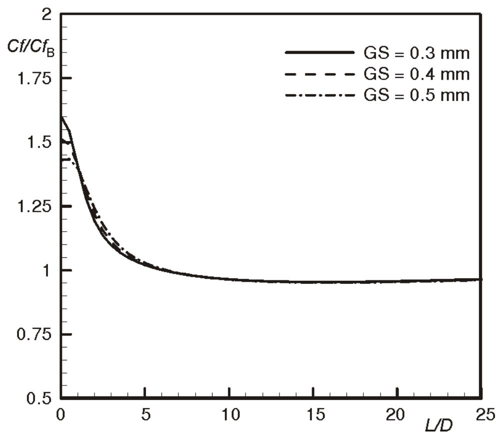

Figure 3. Upstream skin friction distribution for different grid spacing (GS)

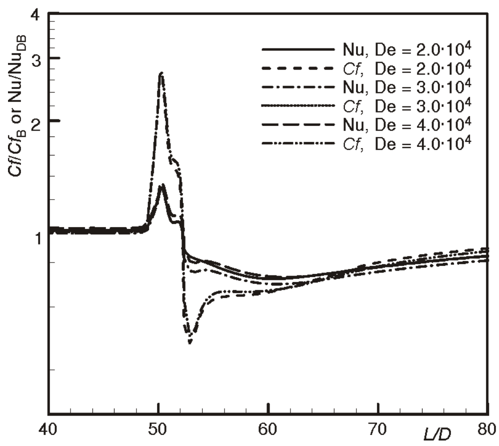

Figure 4. Skin friction and Nusselt number distributions along the inner wall (y-z plane)

certainty in the Dittus-Boelter correlation [12], assumed to be 5%.

Results and discussion

Distributions of skin friction and Nusselt number along the inner wall in the y-z plane are depicted in fig. 4 for different Dean numbers. As shown for *L/D* between roughly 50 and 60, there is a significant influence of the tube curvature on local skin friction and Nusselt number. Downstream of the curvature, both the skin friction and Nusselt number are shown to decrease compared to fully-developed values obtained by the Blasius and Dittus-Boelter correlations for straight pipe. The drawback on heat transfer efficiency downstream of the curvature is due to the centrifugal force in the curved section, and will be shown to limit the overall heat transfer in the tube significantly. Effect of the Dean number in the range of study is shown to be small.

Distributions of skin friction and Nusselt number along the outer wall in the y-z plane are shown in fig. 5 for different Dean numbers. Again, significant influence of the tube curvature on both skin friction and Nusselt number is observed. Downstream of the curvature, both the skin friction and Nusselt number are shown to increase with respect to the developed flow in the straight pipe.

Distribution of the temperature along the wall in the y-z plane is depicted in fig. 6. As expected, the normalized temperature converges to a constant value in the fully-developed region upstream of the curvature. This is also observed downstream of the curvature. However, and unlike upstream where they overlap, the inner wall temperature consistently remains above that of the outer wall throughout the section downstream. The higher inner wall temperature reflects the relatively lower heat transfer rate through the inner wall as depicted in fig. 4. Again,

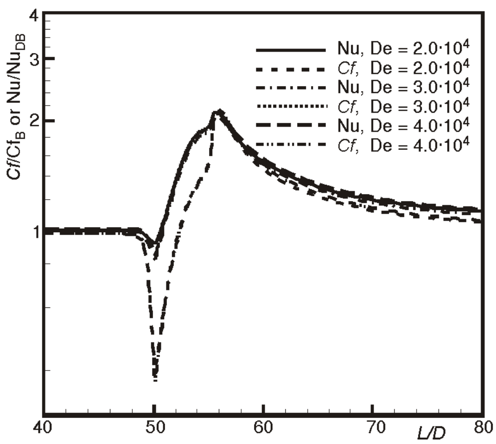

Figure 5. Skin friction and Nusselt number distributions along the outer wall (y-z plane)

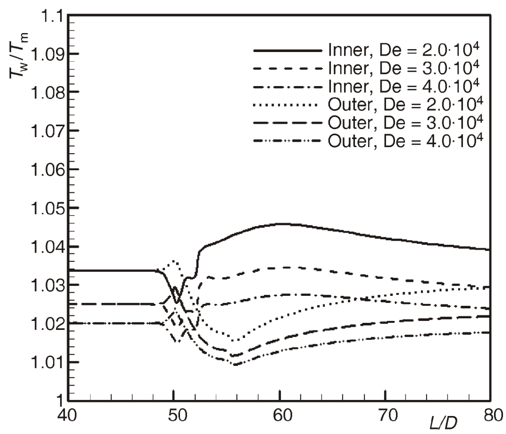

Figure 6. Temperature distribution along the wall (y-z plane)

this difference in the inner and outer wall profiles downstream is due to the secondary motion within the curvature as shown in fig. 7.

Velocity vectors at the mid-section of the curved tube in the x-z plane are shown in fig. 7 for different Dean numbers. Clearly, the secondary motion is shown to increase with increasing Dean number, and is shown to be more significant in the outer wall. It is this variation in velocity profiles that influences flow and heat transfer characteristics within and downstream of the curved sections.

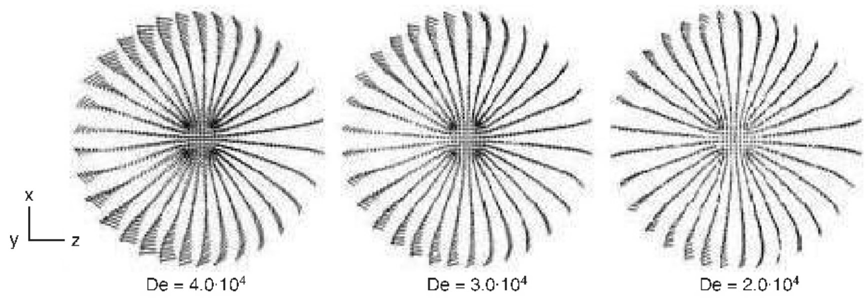

Figure 7. Velocity vectors at the mid-section of the curved tube (x-z plane)

The area-averaged friction factor and Nusselt number for different Dean numbers are shown in tab. 1. The Dean number in the range of study has no effect in the overall skin friction, while the Nusselt number has shown negligible increase with the Dean number. While the Dean number is known to enhance heat transfer in spiral or helical tubes, in U-tubes, such favorable effect is restricted within the curved sections, the area of which are typically small compared to the straight sections upstream and downstream of the curvature. Consequently, the overall heat transfer downstream of the curvature was reduced by 50% compared to a straight pipe, resulting in an overall reduction of 25%. This is a major drawback in U-tube performance since U-tubes are typically used in high performance industrial applications.

Table 1. Area-averaged friction factor and Nusselt number for different Dean numbers

De	$2.0 \cdot 10^4$	$3.0 \cdot 10^4$	$4.0 \cdot 10^4$
Cf_{up}/Cf_B	1.00	1.00	1.00
Cf_{cr}/Cf_B	1.45	1.46	1.45
Cf_{dn}/Cf_B	1.03	1.04	1.05
Cf_a/Cf_B	**1.03**	**1.03**	**1.03**
Nu_{up}/Nu_{DB}	1.00	1.00	1.00
Nu_{cr}/Nu_{DB}	0.98	1.01	1.03
Nu_{dn}/Nu_{DB}	0.48	0.52	0.54
Nu_a/Nu_{DB}	**0.75**	**0.77**	**0.78**

Conclusions

Using the standard k-ε model, turbulent flow and heat transfer characteristics in U-tubes were investigated. The simulation revealed secondary flow within the curved section of the tube. Increasing the Dean number was shown to increase the intensity of the secondary flow. The overall heat transfer downstream of the curvature was shown to decrease significantly compared to straight pipes. No curvature effects on the overall friction factor were predicted. This study shows that the standard k-ε model can be used to investigate flow and heat transfer characteristics in curved tubes.

Acknowledgment

This research was funded by the Research Center of the College of Engineering, King Saud Universuty under grant # 429/65.

Nomenclature

c_p	–	specific heat at constant pressure, [kJkg^{-1}K^{-1}]
De	–	Dean number [= Re$(r/R)^{0.5}$], [–]
E	–	specific energy, [Jkg^{-1}]
Cf_B	–	Blasius correlation for straight pipe (= 0.079 Re$^{-0.25}$), [–]
Cf	–	friction factor [= $\tau_w/(0.5\rho U_a^2)$], [–]
h	–	heat transfer coefficient [= $q/(T_w - T_m)$], [Wm^{-2}K^{-1}],
k	–	turbulence kinetic energy, [m^{2}s^{-2}]
K	–	fluid thermal conductivity, [Wm^{-1}K^{-1}]
L	–	distance along the tube, [m]
Nu	–	Nusselt number (= hD/k), [–]
$\mathrm{Nu_{DB}}$	–	Nusselt number obtained by Dittus--Boelter correlation (= 0.023 Re$^{4/5}$Pr$^{0.4}$), [–]
p	–	mean pressure of the fluid, [Pa]
Pr	–	molecular Prandtl number (= 0.74), [–]
$\mathrm{Pr_t}$	–	turbulent Prandtl number (= 0.85), [–]
q	–	heat flux through the wall, [Wm^{-2}]
r	–	tube radius (= 10 mm)
Re	–	Reynolds number (=$\rho U_a D/m$), [–]
T	–	wall temperature, [K]
T_m	–	$4xq/(\mathrm{Re}\mu C_p) + T_{in}$, [K]
U	–	mean velocity of the fluid, [ms^{-1}]
U_a	–	area-averaged velocity, [ms^{-1}]
x_i	–	Cartesian coordinates

Greek letters

δ_{ij}	–	Kronecker delta
ε	–	turbulence dissipation rate, [m^{2}s^{-3}]
μ	–	dynamic viscosity of the fluid, [kgm^{-1}s^{-1}]
μ_t	–	eddy viscosity, [kgm^{-1}s^{-1}]
ρ	–	mean density of the fluid, [kgm^{-3}]
τ_w	–	wall shear stress, [Pa]

Subscripts

a	–	area-averaged
cr	–	curved section
dn	–	downstream
in	–	tube inlet conditions
up	–	upstream
w	–	parameter at the wall

References

[1] Naphon, P., Wongwises, S., A Review of Heat Transfer and Flow Characteristics in Curved Tubes, *Renewable and Sustainable Energy Reviews, 10* (2006), 5, pp. 463-490
[2] Hüttl, T. J., Wagner, C., Friedrich, R., Navier-Stokes Solutions of Laminar Flows Based on Orthogonal Helical Coordinates, *International Journal of Numerical Methods in Fluids, 29* (1999), 7, pp. 749-763
[3] Galdi, G. P., Robertson, A. M., On Flow of a Navier-Stokes Fluid in Curved Pipes, Part I: Steady Flow, *Applied Mathematics Letters, 18* (2005), 10, pp. 1116-1124
[4] Friedrich, R., *et al.*, Direct Numerical Simulation of Turbulent Flows in Curved and Helically Coiled Pipes, *Computers and Fluids, 30* (2001), 5, pp. 591-605
[5] Li, L. J., Lin, C. X., Ebadian, M. A., Turbulent Mixed Convective Heat Transfer in the Entrance Region of a Curved Pipe with Uniform Wall-Temperature, *Int. J. Heat Mass Transfer, 41* (1998), 23, pp. 3793-805
[6] Yang, R., Chiang, F. P., An Experimental Heat Transfer Study for Periodically Varying-Curvature Curved-Pipe, *Int. J. Heat Mass Transfer, 45* (2002), 15, pp. 3199-3204
[7] Hinze, J. O., Turbulence, McGraw-Hill Publishing Co., New York, USA, 1950
[8] Launder, B. E., Spalding, D. B., Lectures in Mathematical Models of Turbulence. Academic Press, London, 1972, pp. 90-110
[9] Patankar, S. V., Spalding, D. B., A Calculation Procedure for Heat, Mass, and Momentum Transfer in Three-Dimensional Parabolic Flows, *Int. J. Heat and Mass Transfer, 15* (1972), pp. 1787-1806
[10] Sharov, D., Nakahashi, K., Hybrid Prismatic/Tetrahedral Grid Generation for Viscous Flow Applications, *AIAA Journal, 36* (1998), 2, pp. 157-162

[11] Stern, F., *et al*., Verification and Validation of CFD Simulations, Iowa Institute of Hydraulic Research IIHR 407, College of Engineering, University of Iowa, Iowa City, Ia., USA, 1999
[12] Kakac, S., Yener, Y., Convective Heat Transfer, 2nd ed., CRC Press, Boca Raton, Fla., USA, 1995

Author´s affiliation:

K. N. Alammar
Department of Mechanical Engineering,
King Saud University
P. O. Box 800, Riyadh 11421,
Saudi Arabia
E-mail: alammar@ksu.edu.sa

Paper submitted: May 25, 2008
Paper revised: October 1, 2008
Paper accepted: November 11, 2008